The Fiber-Coating Model of Biopharmaceutical Depth Filtration

Glen R. Bolton, Daniel LaCasse, Matthew J. Lazzara, and Ralf Kuriyel
Millipore Corporation, Bedford, MA 01730

DOI 10.1002/aic.10541
Published online August 3, 2005 in Wiley InterScience (www.interscience.wiley.com).

Depth filters are often used in biotechnology processes to remove cell debris from cell culture solutions. A model of filter plugging was developed to allow predictions of required filter area from limited amounts of initial data. The filter microstructure was idealized as an assembly of randomly oriented, straight, cylindrical fibers. It was assumed that filters plug as solids coat the surfaces of fibers, making them thicker and reducing filter porosity and permeability. The Carman–Kozeny equation was used to allow calculation of filter permeability as a function of filter fiber radius, filter solid fraction, and volume filtered. An explicit equation for filtrate volume as a function of time during constant pressure operation was derived, and an explicit equation for pressure as a function of time during constant flow rate operation was derived. A second model that accounted for the combined effects of fiber coating and surface caking was also derived. The models were tested on data from a replica cell culture fluid filtered through a glass fiber based depth filter and data from E. coli lysate filtered through glass fiber and diatomaceous earth based depth filters. The fiber coating model provided good fits of the volume vs. time data and good predictions of filter capacity from limited initial data. The combined cake-fiber coating model provided improved performance over the fiber coating model. The models are useful tools for sizing of depth filters for fermentation and cell culture applications and may be useful for other liquid and gas filter applications. © 2005 American Institute of Chemical Engineers *AIChE J,* 51: 2978–2987, 2005
Keywords: bioseparations, membrane separations, depth filter, fouling, sizing

Introduction

A wide range of processes utilize filters to remove particles from aqueous solutions. Depth filters are often used in biotechnology processes to remove cell debris and other particulates. The filter area required by these applications can either be determined by filter permeability or filter capacity. Filter capacity is an indication of how much volume can be filtered before plugging occurs. Capacity during constant pressure operation is defined as the amount of fluid per filter area that can be processed until the flow rate declines to a set fraction of the initial flow. Capacity under fixed flow rate conditions is determined when the pressure increases to some set multiple of the initial value. Fouling of a filter can occur by deposition of particles inside or on top of the filter.[1,2] There are four mechanistic models that are typically used to describe fouling. Complete blocking assumes that particles seal off pore entrances and prevent flow. Intermediate blocking is similar to complete blocking but assumes that a portion of the particles seal off pores and the rest accumulate on top of other deposited particles. Cake filtration occurs when particles accumulate on the surface of a filter in a permeable cake of increasing thickness that adds resistance to flow. Standard blocking assumes that particles accumulate inside filters on the walls of straight cylindrical pores. As particles are deposited, the pores become constricted and the permeability of the filter is reduced. This model was developed by Hermans and Bredee[3] and has typically been applied to the fouling of microporous filters.[4]

Correspondence concerning this article should be addressed to G. Bolton at Glen_Bolton@millipore.com.

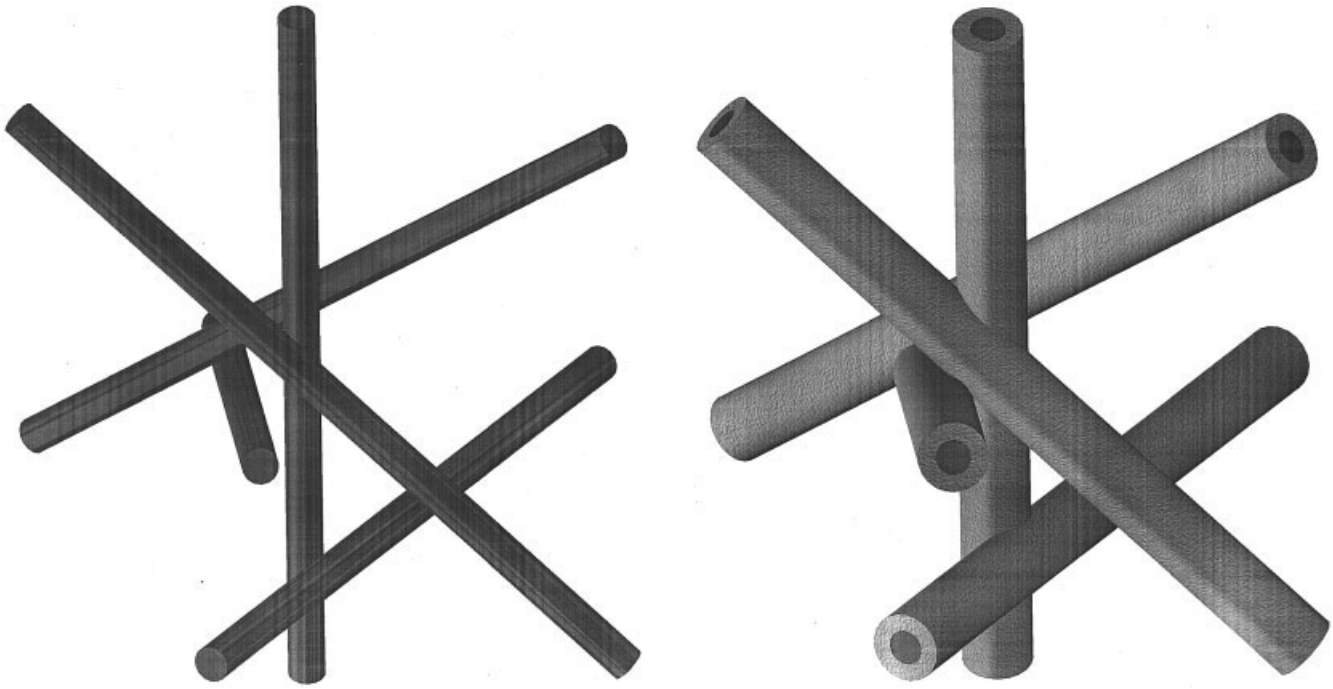

Figure 1. Illustration of a filter composed of randomly oriented fibers before (left) and after (right) plugging.

The filters plug as solids coat the surfaces of fibers, increasing fiber thickness and reducing filter permeability.

The physical assumptions in the classical blocking models are not representative of most depth filters and are therefore not widely used. The straight cylindrical pore microstructure assumed in the classical models does not represent the fibrous structure of most depth filters. Cake can form above depth filters but the pore blockage and pore constriction models do not accurately describe the mechanisms of depth filter fouling. Depth filters are typically fouled by various mechanisms of deposition of particles on the internal surfaces of the media.[5]

In this work an alternative model that treats filters as random fiber matrices was developed. The model predicts a decrease in filter permeability as solids from the process stream deposit on the filter fibers. This deposition increases the effective radius of the fibers and decreases the filter void fraction. A combined model that accounts for cake formation and fiber coating occurring simultaneously was also developed. The models provided good fits of volume vs. time data during filtration and made accurate predictions of filter capacities from limited initial data.

Theory

Fiber coating model

A model of internal filter plugging that treats filters as assemblies of straight cylindrical fibers was developed. It assumes that filters plug as solids coat the surfaces of fibers, making them thicker and reducing filter permeability. This is illustrated in Figure 1.

The model was developed by first relating the fiber radius to the volume of solids removed in a manner similar to that of the standard blocking model[1]

$$L_F 2\pi r_f dr_f = \left(\frac{c}{1-\varepsilon}\right) A dV \tag{1}$$

$$\pi L_F (r_f^2 - r_{f0}^2) = \left(\frac{c}{1-\varepsilon}\right) AV \tag{2}$$

where r_f is the fiber radius, L_F is the total length of all fibers, c is the volume of solids per unit of filtrate volume, ε is the porosity of solid when deposited on the fibers, and V is the volume processed, normalized by filter area A. The filter solid fraction ϕ is related to the fiber radius, filter thickness L_M, and other parameters.

$$\frac{\pi r_{f0}^2 L_F}{L_M A} = \phi_0 \tag{3}$$

The subscript "0" is used to indicate an initial value of a given quantity. After fouling has occurred, the new solid fraction can be related to the new fiber radius by

$$\phi = \frac{\pi r_f^2 L_F}{L_M A} = \phi_0 \left(\frac{r_f}{r_{f0}}\right)^2 \tag{4}$$

Although the deposited solids are assumed to be porous in Eq. 2, Eq. 4 assumes the solids are nonporous. This assumption will be accurate if the flow through the deposited solids is minimal. The term $V_{\max}$ describes the amount of solution volume that can be filtered until the filter void volume is completely filled with solids. A new term, the fiber coating constant K_f, is equal to the inverse of $V_{\max}$. By material balance of solids in the filter volume, $V_{\max}$ is calculated as

$$V_{\max} = \frac{1}{K_f} = L_M \left(\frac{1-\varepsilon}{c}\right)(1-\phi_0) \tag{5}$$

Rearranging Eq. 3 to an expression for L_F and substituting into Eq. 2 yields Eq. 6, which allows calculation of r_f and ϕ from V and four physical constants: L_M, c, ε, and ϕ_0. Insertion of Eq. 5 reduces this to two physical constants, K_f and ϕ_0.

$$\frac{r_f^2}{r_{f0}^2} = \frac{\phi}{\phi_0} = \left[1 + \left(\frac{c}{1-\varepsilon}\right)\frac{V}{L_M\phi_0}\right] = \left[1 + \frac{(1-\phi_0)}{\phi_0}K_fV\right] \tag{6}$$

Combining Eq. 6 with a theoretical model that relates hydraulic permeability to fiber radius allows a filter-plugging model to be derived that relates permeability to filtrate volume.

The Carman–Kozeny model,

$$\frac{\kappa}{r_f^2} = \frac{(1-\phi)^3}{20\phi^2} \tag{7}$$

where κ is filter Darcy permeability, was developed by extending a correlation between Reynolds number and friction factor for laminar flow through pipes to flow through porous media.[6] It has also been used to describe flow through fibrous media.[7] The flow rate through a filter (dV/dt) can be calculated from Darcy's Law as

$$\frac{dV}{dt} = \kappa\frac{\Delta P}{\mu L_M} \tag{8}$$

where ΔP is the transmembrane pressure and μ is the solution viscosity.

In this study it was found that the Carman–Kozeny model was ideal for use in the fiber coating model of filter plugging. As described in more detail in Appendix A, the Carman–Kozeny model accurately represented both rigorous theoretical predictions and a large amount of experimental data over the relevant range of fiber volume fractions.

Fiber coating model: constant pressure

To obtain the equations for the fiber coating model, Eq. 6 can be substituted into Eqs. 7 and 8 to yield flux as a function volume for filtration experiments run at constant pressure

$$\frac{dV}{dt} = \left(\frac{\Delta P}{\mu L_M}\right)\frac{r_f^2(1-\phi)^3}{20\phi^2} = \frac{J_0(1-K_fV)^3}{\left[1 + \frac{(1-\phi_0)}{\phi_0}K_fV\right]} \tag{9}$$

where J_0 is the initial solvent flux. The equation can be integrated to obtain an explicit equation for filtrate volume as a function of time

$$V = \frac{1}{K_f} + \frac{1}{K_f\alpha}\left[1 - \sqrt{1 + \frac{\alpha}{(1-\phi_0)}}\right] \tag{10}$$

where α is a dimensionless parameter, defined as

$$\alpha = (2K_fJ_0t + 1)\left(\frac{\phi_0}{1-\phi_0}\right) - 1 \tag{11}$$

To determine the filtrate volume as a function of percentage flux decline, such as the volume after the flux has declined 75% from its initial value, it is necessary to solve for the roots of Eq. 9. The real root of this cubic polynomial can be calculated using Cardan's formula[8]

$$V = \frac{1}{K_f}\left(1 - \sqrt[3]{\chi + \sqrt{\delta}} + \sqrt[3]{-\chi + \sqrt{\delta}}\right) \tag{12}$$

where β, χ, and δ are placeholders defined, respectively, as

$$\beta = \frac{(1-\phi_0)}{3\phi_0}\frac{J}{J_0}$$

$$\chi = \frac{1}{2\phi_0}\frac{J}{J_0}$$

$$\delta = \beta^3 + \chi^2$$

Fiber coating model: constant flow

For filtration experiments run at a constant flux, Eq. 9 can be rearranged to obtain an explicit expression for pressure as a function of time, where $V = J_0t$

$$\frac{\Delta P}{\Delta P_0} = \frac{\left[1 + \frac{(1-\phi_0)}{\phi_0}K_fV\right]}{(1-K_fV)^3} \tag{13}$$

This model is similar to a model of increasing pressure drop with deposition of solids on packed spheres.[5] To determine the filtrate volume as a function of relative pressure increase, such as the volume after the pressure has increased tenfold from the initial value, Eq. 12 can be used, where the parameters β and χ will now be defined, respectively, as

$$\beta = \frac{(1-\phi_0)}{3\phi_0}\frac{\Delta P_0}{\Delta P}$$

$$\chi = \frac{1}{2\phi_0}\frac{\Delta P_0}{\Delta P}$$

Equations 10 and 13 were derived assuming that fibers never overlapped and all solids deposited evenly along the fibers. It is possible, however, to have fibers that intersect or have a significant portion of their surface area in contact with one another. In this case the fiber radius will increase with permeate volume faster than that described by Eq. 6 because the solids will deposit on fiber surfaces only where there is no contact or overlap. Equations 10 and 13 are corrected for fiber overlap in Appendix B. In practice filters typically will have characteristics that are between the cases of overlapping and nonoverlapping fibers. For the glass fibers used in this study there will be fiber contacting and but no overlap initially. Once solids are deposited, however, the coated fibers will overlap at the points where the fibers were initially in contact. This is illustrated in Figure 1. The sizing predictions in this study were not significantly changed by accounting for the effects of fiber overlap.

Combined cake-fiber coating model

Typically foulants accumulate throughout the thickness of depth filters. Large foulants such as intact cells, however, can accumulate as cakes above filters. To account for the effects of these cakes, the fiber coating model was modified by adding the resistance caused by these cakes. The cake resistance R can be calculated as a function of permeate volume

$$\frac{R}{R_0} = (1 + K_c J_0 V) \tag{14}$$

where K_c is the cake filtration constant and R_0 is the initial filter resistance.[2] For the combined model, the filter resistance increases with permeate volume as the fibers become coated with foulants and, simultaneously, the cake thickness increases with permeate volume. This is similar to recently developed models of the combined effects of the classical fouling modes.[9] Higher K_f or K_c values physically correspond to a larger reduction in filter permeability for a given permeate volume. The flux can be calculated as a function of permeate volume using the following equation, where the total resistance is the sum of the resistances of the fibrous filter and the cake

$$\frac{dV}{dt} = \frac{J_0}{\left\{\left[1 + \frac{(1-\phi_0)}{\phi_0} K_f V\right](1 - K_f V)^{-3} + K_c J_0 V\right\}} \tag{15}$$

Equation 17 can be integrated to calculate time as a function of volume

$$t = \frac{K_c V^2}{2} + \frac{1}{2K_f J_0}\left\{\left[1 + \frac{(1-\phi_0)}{\phi_0}(K_f V)^2\right](1 - K_f V)^{-2} - 1\right\} \tag{16}$$

Equations 17 and 18 reduce to the equations for cake filtration when K_f is small and to the equations for fiber coating when K_c is small. It is difficult to rearrange Eq. 18, a fourth-order polynomial in volume, to calculate volume as a function of time, although Eq. 18 is still useful for fitting experimental data and predicting filter capacities. Typically the experimental values of time are used as inputs to plugging models to calculate volumes. The predicted volumes are then compared to the experimental values to determine the best-fit parameters. The best-fit parameters in Eq. 18 can be determined by using the experimental volume values as inputs and calculating the corresponding time values. The predicted times can then be compared to the experimental values and the parameters K_c and K_f can de determined.

For the case where the filtration experiment is run at a constant flux, Eq. 17 can be rearranged to obtain Eq. 19, which allows explicit calculation of pressure as a function of time, where $V = J_0 t$

$$\frac{\Delta P}{\Delta P_0} = \frac{\left[1 + \frac{(1-\phi_0)}{\phi_0} K_f V\right]}{(1 - K_f V)^3} + K_c J_0 V \tag{17}$$

To determine the filtrate volume as a function of relative pressure increase, such as the volume after the pressure has increased tenfold from the initial value, it is most convenient to solve Eq. 19 numerically.

Experimental

Glass-fiber filter

Filters were composed of glass fibers with a binder resin (AP1504700, Millipore, Bedford, MA). Fiber radii were determined from scanning electron micrographs and filter permeabilities. Samples were sputter coated using a Au/Pd target before SEM analysis. Images were acquired at a 1000× magnification using a Topcon DS-130-C scanning electron microscope. The fibers observed in scanning electron micrographs had radii ranging from 0.2 to 5.0 μm. The filter solid fraction was determined to be 0.07 $\pm$ 0.01 by measuring the volume displacement of the media as follows. Three 47-mm media disks were rolled up and submerged in a 20-mL graduated cylinder containing 18 mL of water. The cylinder was then put in a 1 gallon sonic cleaner (FS30H, Fisher Scientific, Hampton, NH) for 10 min to remove air bubbles and the volume displacement was measured. This was done in triplicate. The media thickness was determined to be 0.54 mm using calipers. The average hydraulic permeability of the media was 9400 L m^{-2} h^{-1}·psi. The effective fiber radius was determined by fitting the initial permeability of the filter using Eq. 16. The effective fiber radius was 0.17 microns, which was at the low end of the range observed in filter SEMs.

E. coli lysate

Plugging experiments were performed with a solution of lysed *Escherichia coli* BL21 cells obtained from Dr. Carl Lawton of the University of Massachusetts, Lowell. The lyaste was obtained frozen at pH 7.0 in a mixture of 50 mM sodium acetate with 2 mM EDTA lysis buffer and PBS media buffer.

Replica cell culture fluid

A fluid representing a clarified solution from a mammalian cell culture vessel was made up of the following components: 13.47 g/L DMEM (D-7777, Sigma, St. Louis, MO), 3.70 g/L $NaHCO_3$ (7412, Mallinckrodt, Hazelwood, MO), 1 g/L Pluronic F-68 (P1300, Sigma), 0.0775 g/L DNA(D6898, Sigma), 5.0 g/L soy peptone fraction IV (P0521, Sigma), 1.5 g/L dairy whey (W1500, Sigma), and 3.00 mg phosphatidylcholine (P3644, Sigma). The feed solution was used within 2 h after preparation to minimize variability.

Filter testing equipment: constant pressure

The plugging solution was contained in a pressure vessel (XX1100000, Millipore). The filter was placed in a 47-mm stainless steel holder (XX4404700, Millipore). An electronic balance aperture and a collection vessel were used to collect and measure the filtrate weight. The electronic balance consisted of a load cell (1042-3-I, Tedea Huntleigh, Covina, CA) that interfaced with a computer through a data-acquisition board.

During constant pressure experiments, the system was pressurized with air and a digital pressure gauge was used

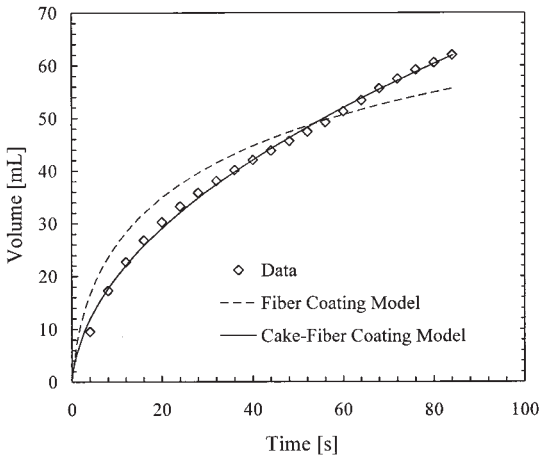

Figure 2. Volume vs. time data compared to the fiber coating and cake-fiber coating model predictions with 10× diluted *E. coli* lysate run at 3 psi through AP15 glass-fiber media.

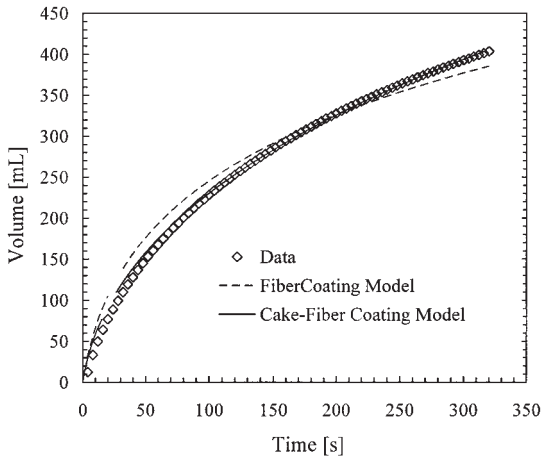

Figure 3. Volume vs. time data compared to the fiber coating and cake-fiber coating model predictions with 100× diluted *E. coli* lysate run at 3 psi through AP15 glass-fiber media.

(2798K12, McMaster-Carr, Atlanta, GA). The 47-mm filter disks were wetted with water and placed in holders. The holders were then connected to 600-mL feed reservoirs. The feed solutions were added to their appropriate chambers and the four chambers were pressurized to 3 psi. The filter holders were vented to remove air. The filtrate valves were then opened and data acquisition began. The filter surface area was 1.38×10^{-3} m^2. Data were collected at 1-s intervals for 1 h.

During constant flow experiments, a three-head peristaltic feed pump (7523-50, 77201-60, Cole Parmer, Vernon Hills, IL) was used with a pressure gauge (XXPXLGAGE, Millipore). The load cell, data acquisition, and filter holder were the same as those used in the constant pressure experiments.

Results

Constant pressure: E. coli lysate on glass fiber

The *E. coli* lysate solution was diluted 10-, 100-, and 1000-fold with pH 7.2 PBS buffer (DF2314-15-0, Fisher) and filtered at a constant pressure through the glass filters. The permeate volume was measured as a function of time until the flux had decreased by 95% from its initial value.

The permeate volume and time data were fit using the fiber coating model, Eq. 10, by varying K_f, and using the cake-fiber coating model, Eq. 18, by varying K_f and K_c. The best fit was determined by minimizing the sum of squared residuals (SSR), where the residual was equal to the difference between an experimental data point and a model prediction. The residual was calculated from volume values for the fiber coating model, and from time values for the cake-fiber coating model. The volume vs. time data are compared to model predictions in Figures 2, 3, and 4 for the different lysate dilutions.

The fiber coating model provided good fits of the *E. coli* lysate data. The solid volume fraction, determined from Eq. 12, increased from the initial value of 0.07 to 0.54 and 0.39 for the streams diluted 10- and 1000-fold, respectively. The cake-fiber coating model provided better fits than the fiber coating model alone. The difference between the fit of the two models increased with decreasing dilution factor. The combined model does benefit from the use of two fitted parameters. It is possible, however, that more cake formed above the filters used with the more concentrated streams, as would be expected, resulting in the improved fit of the combined model. The K_f term was near zero, indicating that the cake model alone provided the best fit for the 10 × diluted stream. Table 1 summarizes the residuals, an indication of quality of fit, and the fitted parameters from the two models for the different streams.

Constant flow rate: replica cell culture fluid on glass fiber

The applicability of the models to data from a constant flow experiment performed with the replica cell culture fluid was tested. The fluid was filtered at a constant flow rate of 2600 L m^{-2} h^{-1} through the AP15 glass media and the pressure was measured. The experiment was performed with the replica cell culture fluid diluted four- and ten fold. The experimental ap-

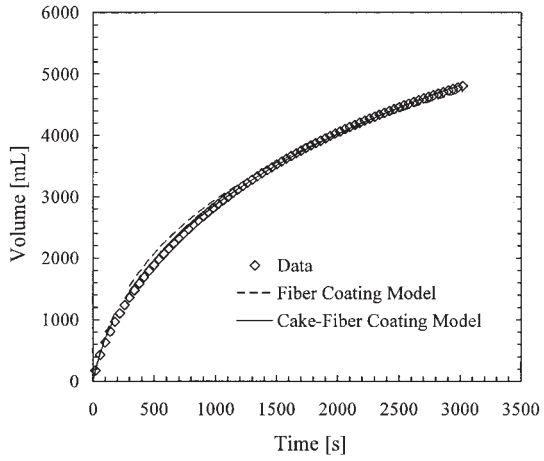

Figure 4. Volume vs. time data compared to the fiber coating and cake-fiber coating model predictions with 1000× diluted *E. coli* lysate run at 3 psi through AP15 glass-fiber media.

Table 1. Error of Fit and Model Parameters for the Fiber Coating and Cake-Fiber Coating Models*

Model	Dilution Factor	Initial Flux, J_0 (m/s)	Model Fit Error, SSR	Fit Parameter Values
Fiber coating model (Eq. 10)	10	7.83×10^{-3}	$4.37 \times 10^{+3}$	$K_f = 1.25 \times 10^{1}$
Cake-fiber coating model (Eq. 18)	10	7.83×10^{-3}	2.63×10^{1}	$K_f = 1.00 \times 10^{-8}$ $K_c = 7.78 \times 10^{4}$
Fiber coating model (Eq. 10)	100	7.83×10^{-3}	2.09×10^{4}	$K_f = 1.39$
Cake-fiber coating model (Eq. 18)	100	7.83×10^{-3}	5.46×10^{2}	$K_f = 9.36 \times 10^{-1}$ $K_c = 3.01 \times 10^{3}$
Fiber coating model (Eq. 10)	1000	7.83×10^{-3}	7.80×10^{5}	$K_f = 9.87 \times 10^{-2}$
Cake-fiber coating model (Eq. 18)	1000	7.83×10^{-3}	3.24×10^{4}	$K_f = 8.16 \times 10^{-2}$ $K_c = 1.02 \times 10^{2}$

*Data for 10,100 and 1000× diluted *E. coli* lysate run at 3 psi through AP15 glass-fiber media.

paratus, filter area, and filter thickness were the same as described previously. The pressure vs. time data were fit to the fiber coating model, Eq. 13, and the cake-fiber coating model, Eq. 19, by minimizing the SSR values. The initial pressure drop was too low to measure accurately. It was estimated to be 0.3 psi by dividing the flux by the filter permeability. The data and model predictions are shown in Figures 5 and 6. Table 2 summarizes the residuals and fitted parameters from the two models.

The fiber coating model provided good fits of the pressure increase observed in the experiments for both the 4 and 10 × diluted replica cell culture fluid stream. The fits were improved by using the combined cake-fiber coating model, although this model does benefit from the use of two fitted parameters. It is possible that in these experiments, similar to the observation in the *E. coli* lysate experiments, more cake formed above the filter used with the more concentrated stream, resulting in the improved fit of the combined model.

Constant flow rate: E. coli lysate on Millistak

The applicability of the models to constant flow data for the filtration of 10 × diluted *E. coli* lysate on commercially available fibrous depth filters was tested. The fluid was filtered at a constant flow rate of 364 L m^{-2} h^{-1} through a Millistak A1HC (MA1HC23HH3, Millipore) disposable depth filter device and the pressure was measured. The filter consisted of about 3 mm of an open grade of cellulose media embedded with diatomaceous earth, followed by 3 mm of a tighter grade, followed by a thin layer of microporous membrane. The fibrous, cellulose-based structure of this media makes it ideal for application of the fiber coating model. The solid fraction of the first layer was determined to be 27%, and the second layer 23%, from measurements of volume displacement using water and a volumetric flask. The solid fraction of the overall filter was taken as 25%, the thickness-weighted average of the two measurements. The pressure vs. time data were fit to the fiber coating model, Eq. 13, by minimizing the SSR values. The best fit of the cake-fiber coating model occurred with K_c near zero and was identical to the fit of the fiber coating model alone. The fiber coating model provided a good fit of the pressure increase observed in the experiment, as shown in Figure 7.

The ability of the fiber coating and cake-fiber coating models to accurately predict filter sizing was evaluated by fitting a limited amount of initial pressure data and then comparing the predicted volume corresponding to a set pressure limit to the experimental data. This is representative of scale-down studies used to estimate area requirements for large-scale filter processes. Generally only limited time and process fluid are available. Extrapolating data from partially plugged filters to higher plugging values using a plugging model can save time, process fluid, and allow more experiments to be performed. Parameters were fit to the initial data and the volume that would be obtained when the pressure reached the final pressure was calculated. The predictions are compared to the actual volumes at the respective final pressures in Figure 8 for the fiber coating model (Eq. 13) and Figure 9 for the cake-fiber coating model (Eq. 19).

The fiber coating model predictions in Figure 8 were within 20% of the experimental data when more than 15% of the full pressure range was used for parameter fitting. This was true for both dilutions of the replica cell culture fluid run on the glass filter and the *E. coli* lysate run on the Millistak media. This indicates the fiber coating model is a useful tool for making accurate filter sizing predictions with heterogeneous depth filtration media based on limited amounts of pressure vs. volume data. Occasionally, fibrous clarification media will be limited by breakthrough of impurities and not by pressure increase as a result of fouling. In this case other criteria such as permeate turbidity will be more important for sizing.

The combined cake-fiber coating model provided some improvement in the accuracy of the capacity predictions. The cake-fiber coating model predictions in Figure 9 were up to 16% closer to the actual values than the fiber coating model for the 10 × diluted replica cell culture fluid, and up to 4% better

Table 2. Error of Fit and Model Parameters for the Fiber Coating and Cake-Fiber Coating Model*

Model	Dilution Factor	Initial Flux, J_0 (m/s)	Model Fit Error, SSR	Fit Parameter Values
Fiber coating model (Eq. 13)	4	7.25×10^{-4}	41.6	$K_f = 2.92$
Cake-fiber coating model (Eq. 19)	4	7.25×10^{-4}	10.7	$K_f = 2.76$ $K_c = 3.75 \times 10^{4}$
Fiber coating model (Eq. 13)	10	7.25×10^{-4}	24.1	$K_f = 1.72$
Cake-fiber coating model (Eq. 19)	10	7.25×10^{-4}	3.43	$K_f = 1.64$ $K_c = 1.49 \times 10^{4}$

*Data for 4 and 10× diluted replica cell culture fluid run at 2600 L m^{-2} h^{-1} through AP15 glass-fiber media.

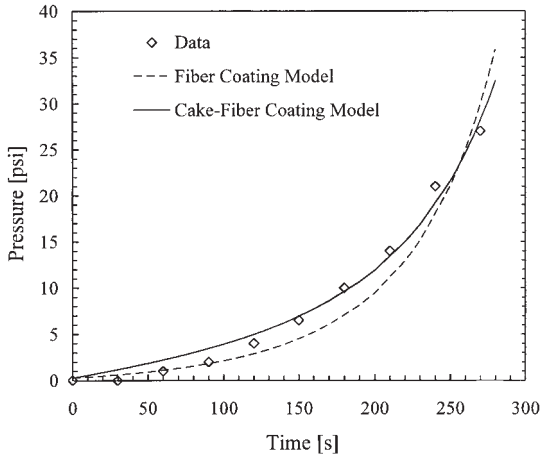

Figure 5. Pressure vs. time data compared to the fiber coating and cake-fiber coating model predictions with 4× diluted replica cell culture fluid run at 2600 L m^{-2} h^{-1} through AP15 glass-fiber media.

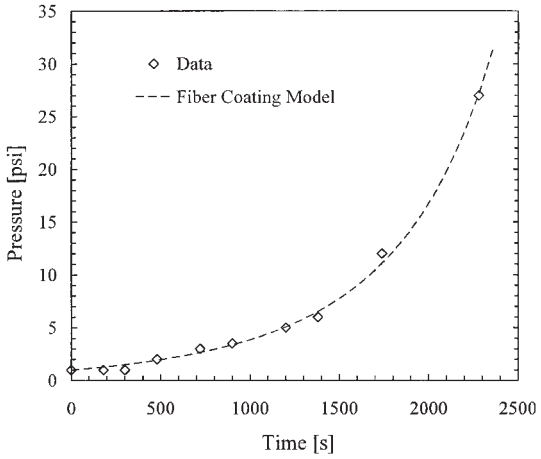

Figure 7. Pressure vs. time data compared to fiber coating model predictions for experiment run at 364 L m^{-2} h^{-1} with 10× diluted *E. coli* lysate on Millistak A1HC depth filter media.

for the 4 × diluted replica cell culture fluid. The combined model did not provide better fits of the *E. coli* lysate data and was not used for capacity predictions. It is likely that the cake-fiber coating model will be more accurate than the fiber coating model for sizing filters in processes where large foulants that accumulate above filters are present.

Conclusions

A model of internal filter plugging that assumed filters were composed of straight cylindrical fibers was developed. The model relates the volume filtered to the filter solid fraction and fiber thickness by assuming that all plugging solids coated the fibers and increased the filter solid fraction. The Carman–Kozeny equation was used with Darcy's Law to calculate flux as a function of volume filtered. The flux equation was integrated to derive an explicit equation for filtrate volume as a function of time when operating at constant pressure. An explicit equation for pressure as a function of time when operating at a constant flow rate was also derived. A second model that accounts for the combined effects of fiber coating and cake formation was also developed.

The models were tested by filtering different dilutions of an *E. coli* lysate through filters composed of glass fibers at constant pressure. The fiber coating model provided good fits of data from constant pressure experiments run with *E. coli* lysate on glass filters. The fiber coating model made accurate filter capacity predictions using limited pressure vs. time data for constant flow fouling of glass filters by the replica cell culture fluid and commercially available depth filtration media by *E. coli* lysate. The cake-fiber coating model provided improved

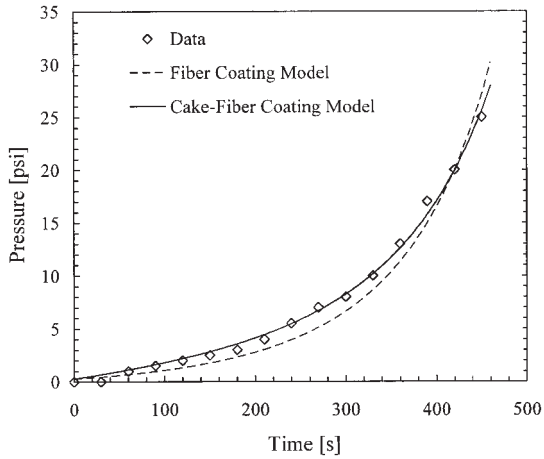

Figure 6. Pressure vs. time data compared the fiber coating and cake-fiber coating model predictions with 10× diluted replica cell culture fluid run at 2600 L m^{-2} h^{-1} through AP15 glass-fiber media.

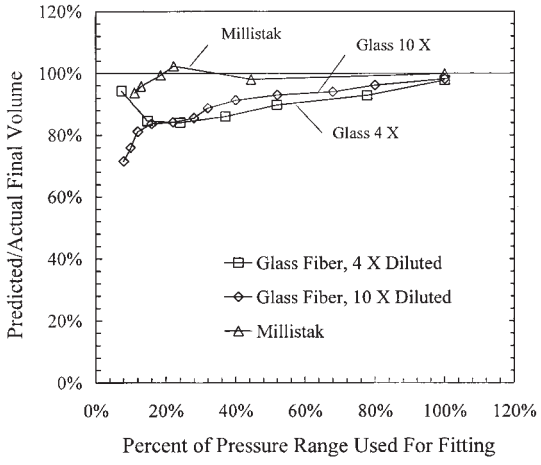

Figure 8. Accuracy of capacity predictions from the fiber coating model.

Predicted final volume normalized by actual final volume as a function of percentage of pressure range used to determine parameter values. Data for the 4 and 10× diluted replica cell culture fluid run at 2600 L m^{-2} h^{-1} through AP15 glass-fiber media, and 10× diluted *E. coli* lysate on Millistak A1HC depth filter media run at 364 L m^{-2} h^{-1}.

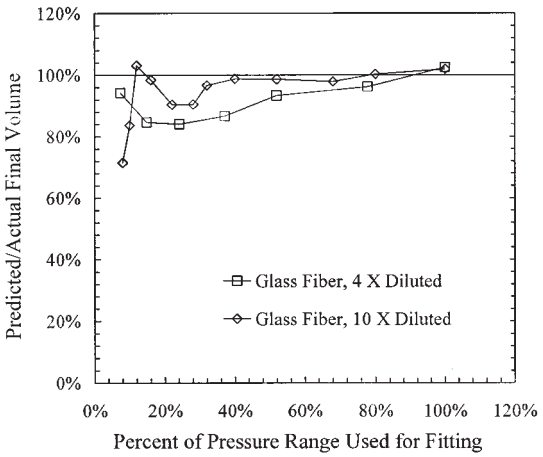

Figure 9. Accuracy of capacity predictions from the cake-fiber coating model.

Predicted final volume normalized by actual final volume as a function of percentage of pressure range used to determine parameter values. Data for the 4 and 10× diluted replica cell culture fluid run at 2600 L m^{-2} h^{-1} through AP15 glass fiber media.

volume vs. time fits and improved sizing predictions. The improvement was greatest for concentrated streams where it is possible cakes formed above the filters. The fiber coating model and cake-fiber coating models will be useful tools for the sizing of depth filtration media used in biotechnology and potentially for other types of fibrous filters used with both liquids and gases.

Acknowledgments

The authors thank Dave Yavorsky, Carl Lawton, Ven Raman, Oleg Shinkazh, John Royce, and Matthew Tomasko for providing the filters, the replica cell culture fluid, and the *E. coli* lysate, and Robin de la Parra for taking the SEM images.

Notation

A = total filter area, m^2
c = volume of solids per unit of filtrate volume
K_c = cake filtration constant, s/m^2
K_f = fiber coating constant, 1/m
L_F = total fiber length, m
L_M = filter thickness, m
P = pressure, kg/ms^2
J = solvent flux, m/s
r_f = fiber radius, m
t = time, s
V = volume filtered, m^3/m^2
V_{max} = maximum volume filtered, m^3/m^2

Greek letters

α = dimensionless placeholder in Eq. 10
β = dimensionless placeholder in Eq. 12
χ = dimensionless placeholder in Eq. 12
δ = dimensionless placeholder in Eq. 12
ε = porosity of deposited solids
ϕ = filter solid or fiber volume fraction
κ = Darcy permeability, m^2
μ = solution viscosity, kg/ms

Literature Cited

1. Grace HP. Structure and performance of filter media. *AIChE J.* 1956; 2:307-336.
2. Hermia J. Constant pressure blocking filtration laws—Application to power-law non-Newtonian fluids. *Trans IChemE.* 1982;60:183-187.
3. Hermans PH, Bredee HL. Principles of the mathematical treatment of constant-pressure filtration. *J Soc Chem Ind.* 1936;55T:1-4.
4. Badmington F, Wilkins R, Payne M, Honig ES. V_{max} testing for practical microfiltration train scale-up in biopharmaceutical processing. *Biopharm.* 1995;Sep.:46-52.
5. Tien C. *Granular Filtration of Aerosols and Hydrosols*. Stoneham, MA: Butterworth; 1989.
6. Carman PC. Fluid flow through granular beds. *Trans IChemE.* 1937; 15:150-166.
7. Sullivan RR, Hertel KL. The flow of air through porous media. *J Appl Phys.* 1940;11:761-765.
8. Nickalls RWD. A new approach to solving the cubic: Cardan's solution revealed. *Math Gazette.* 1993;77:354-359.
9. Bolton GR, LaCasse D, Kuriyel R. Combined models of membrane fouling: Development and application to microporous and ultraporous membranes. *J Membr Sci.* 2005; in press.
10. Ogston AG. The spaces in a uniform random suspension of fibers. *Trans Faraday Soc.* 1958;54:1754-1757.
11. Bolton GR, Deen WM. Limitations in the application of fiber-matrix models to glomerular basement membrane. In: Layton HE, Weinstein AM, eds. *Membrane Transport and Renal Physiology* (IMA Series: Mathematics and Its Application). New York, NY: Springer-Verlag; 2001:141-156.
12. Jackson GW, James DF. The permeability of fibrous porous media. *Can J Chem Eng.* 1986;64:364-374.
13. Higdon JJL, Ford GD. Permeability of three-dimensional models of fibrous porous media. *J Fluid Mech.* 1996;308:341-361.
14. Clague DS, Kandhai BD, Zhang R, Sloot PMA. Hydraulic permeability of (un)bounded fibrous media using the lattice Boltzmann method. *Phys Rev E.* 2000;61:616-625.

Appendix A

There are a number of theoretical models that relate filter permeability to fiber radius and fiber volume fraction.[11] Jackson and James[12] modeled the hydraulic permeability of a random fibrous filter using a cubic array of cylindrical rods. The resistance to flow was the sum of that arising from the rods aligned parallel and perpendicular to the direction of flow. Permeability data were reviewed for materials with a wide range of fiber radii and fiber volume fractions. The model fit the data well for fiber volume fractions < 0.2.

Higdon and Ford[13] obtained numerical solutions to flow around three-dimensional fibrous media using the spectral boundary element method. They obtained results for a wide range of filter solid fractions using slender-body theory at low fiber concentrations and the lubrication approximation at high fiber concentrations. Their results agreed with the data reviewed in Jackson and James[12] for fiber volume fractions between 0.0309 and 0.865.

Clague et al.[14] used a Lattice–Boltzman simulation method to make numerical calculations of the Darcy permeability of a disordered, three-dimensional array of cylinders. Their results (presented in their Figure 8) also fit the data in Jackson and James[12] and agreed with the face-centered cubic fiber lattice predictions of Higdon and Ford[13] for fiber volume fractions between 0.05 and 0.7.

The Carman–Kozeny model,

$$\frac{\kappa}{r_f^2} = \frac{(1-\phi)^3}{20\phi^2} \tag{A1}$$

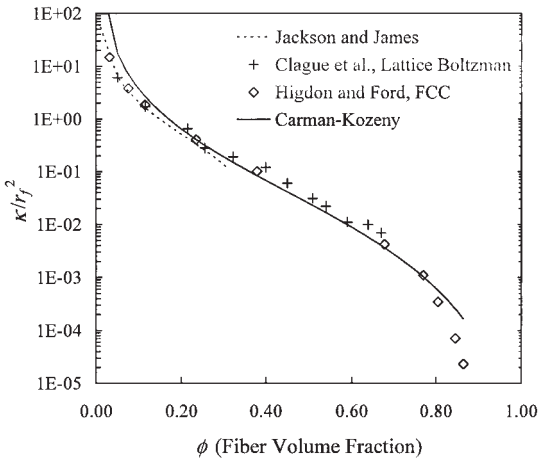

Figure A1. Hydraulic permeability as a function of fiber volume fraction.

The permeabilities calculated with the Carman–Kozeny model are compared to those calculated with the Jackson and James model[12] and with the numerical calculations of Higdon and Ford[13] and Clague et al.[14]

where κ is filter Darcy permeability, was developed by extending a correlation between Reynold's number and friction factor for flow through pipes to flow through porous media.[5] It has also been used to describe flow through fibrous media.[6] The flow through a filter can be calculated from Darcy's Law:

$$\frac{dV}{dt} = \kappa \frac{\Delta P}{\mu L_M} \tag{A2}$$

In this study the Carman–Kozeny model predictions were compared to the numerical results of Higdon and Ford[12] and Clague et al.[13] The Carman–Kozeny equation provided good agreement with the results from the other two studies. A comparison of the models is shown in Figure A1.

The predictions of the Carman–Kozeny were within 50% of the Higdon and Ford predictions for fiber volume fractions between 0.1 and 0.8. This range is typical of the majority of fibrous media. For low fiber volume fractions, between 0.05 and 0.1, the Carman–Kozeny predictions were higher by less than a factor of two.

In Figure A2 the predictions of the Carman–Kozeny model are compared to the experimental data summarized by Jackson and James.[11] The Carman–Kozeny model fit the majority of the experimental data. The predictions were within the scatter of the summarized data for volume fractions above about 0.05. At volume fractions < 0.05 the model overpredicted the data. This indicates the Carman–Kozeny model can be used as a simple mathematical flux equation that accurately represents both rigorous theoretical predictions and a large amount of experimental data.

Appendix B

Equations 10 and 13 were derived assuming that fibers never overlapped and all solids deposited evenly along the fibers. It is possible, however, to have filters with fibers that intersect or have a significant portion of their surface area in contact with one another. In this case the fiber radius will increase with permeate volume faster than as described by Eq. 6 because the solids will deposit on fiber surfaces only where there is no contact or overlap with another fiber.

The following derivation corrects the fiber coating model for the effects of fiber overlap both initially and as the fibers grow uniformly in radius. The filter is assumed to be composed of fibers that are randomly distributed with respect to one another. One consequence of the assumption of randomness is that fibers in this hypothetical matrix will overlap with one another. Thus, the true solid volume fraction of the filter cannot be calculated directly using the number concentration of fibers and the volume of an individual fiber. For completely nonintersecting fibers, the solid volume fraction varies as r_f^2 and ϕ is related to ϕ_0 as

$$\phi = \phi_0 \left(\frac{r_f}{r_{f0}} \right)^2 \tag{B1}$$

For any random-fiber matrix with a nominal value of ϕ, the true solid volume fraction ϕ^* can be calculated by considering the partitioning of a point-sized particle in that matrix. As a solute becomes infinitely small, the fraction of the filter volume from which it is excluded is equal to the true solid volume fraction of the filter. The partition coefficient (Φ) for such a solute is given by

$$\Phi = 1 - \phi^* \tag{B2}$$

To relate ϕ^* to ϕ, we consider now the classical result of Ogston[10] for the partitioning of rigid spherical solutes in random-fiber matrices, wherein no specific accounting for fiber intersection is made. The Ogston result relates Φ to the solute radius r_s, fiber radius r_f, and nominal fiber solid volume fraction ϕ, as

$$\Phi = \exp\left[-\phi \left(1 + \frac{r_s}{r_f} \right)^2 \right] \tag{B3}$$

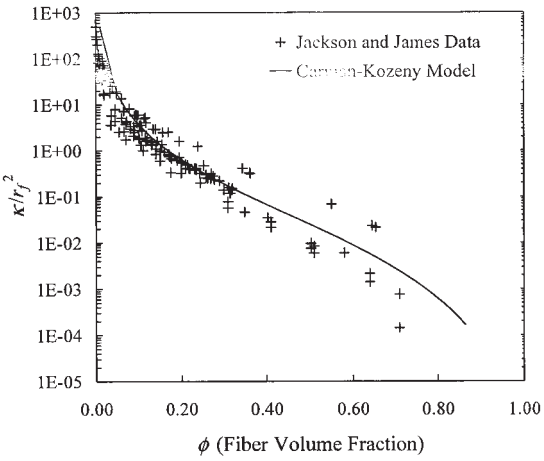

Figure A2. Hydraulic permeability as a function of fiber volume fraction.

The permeabilities calculated with the Carman–Kozeny model are compared to the experimental data summarized in the Jackson and James review.[12]

As $r_s \rightarrow 0$, the Ogston result reduces to $\exp(-\phi)$. Equating Eqs. B2 and B3,

$$1 - \phi^* = \exp(-\phi) \tag{B4}$$

In the fibrous filter the true solid volume fraction will increase as solids are deposited according to

$$V\left(\frac{c}{1-\varepsilon}\right) = L_M(\phi^* - \phi_0^*) \tag{B5}$$

The maximum volume that can be filtered or $V_{\max}$ will be described by

$$V_{\max} = L_M\left(\frac{1-\varepsilon}{c}\right)(1 - \phi_0^*) \tag{B6}$$

Inserting Eq. B6 into B5 yields

$$\phi^* = (1 - \phi_0^*)\frac{V}{V_{\max}} + \phi_0^* \tag{B7}$$

The fiber radius will increase faster with a given change in true solid volume fraction than an equivalent change in nominal solid volume fraction. The fiber radius can be related to the true solid volume fraction by inserting Eq. B4 into Eq. 4.

$$\frac{\phi}{\phi_0} = \frac{\ln(1-\phi^*)}{\ln(1-\phi_0^*)} = \left(\frac{r_f}{r_{f0}}\right)^2 \tag{B8}$$

An equation for flux as a function of true solid volume fraction can be obtained by inserting Eq. B8 for fiber radius into the Carman–Kozeny equation:

$$\frac{dV}{dt} = \left(\frac{\Delta P}{\mu L_M}\right)\frac{r_f^2(1-\phi^*)^3}{20\phi^{*2}} = J_0\frac{\ln(1-\phi^*)}{\ln(1-\phi_0^*)}\left(\frac{\phi_0^*}{\phi^*}\right)^2\left(\frac{1-\phi^*}{1-\phi_0^*}\right)^3 \tag{B9}$$

An equation for flux as a function of volume can be obtained by inserting the equation relating true solid volume fraction to permeate volume, Eq. B7, into Eq. B9. This can be solved numerically for volume vs. time at different values of the parameter $V_{\max}$.

The fibers will be thicker for a given change in solid volume fraction when accounting for the fiber overlap. Solids will deposit more on the ends of fibers where there is no overlap than in centers where the surface area is unavailable. The flux increases with the square of fiber radius in Eq. B9. For a single solid fraction value, the flux will be higher when the fiber radius is larger. It will thus require a larger amount of solids to cause a similar flux decline when accounting for fiber overlap.

An equation similar to B9 can be derived for constant flow conditions, as follows:

$$\frac{\Delta P}{\Delta P_0} = \frac{\ln(1-\phi_0^*)}{\ln(1-\phi^*)}\left(\frac{\phi^*}{\phi_0^*}\right)^2\left(\frac{1-\phi_0^*}{1-\phi^*}\right)^3 \tag{B10}$$

An explicit equation for calculation of pressure as a function of time or volume can be obtained by inserting the equation relating the true fiber volume fraction to permeate volume, Eq. B7, into Eq. B10.

The effect of the overlap on the predicted filter capacities in Figure 8 was determined. The predictions made using Eq. B10 were within 1% of the fiber coating model for the 10 × diluted replica cell culture fluid run on glass filters and the *E. coli* lysate run on Millistak. The overlap model predictions were up to 4% better for the 4 × diluted replica cell culture fluid run on glass filters. The effect of overlap is not expected to significantly alter the capacity predictions. In cases where it is important, Eq. B10 can be used to calculate filter capacities numerically.

Manuscript received Sep. 3, 2004, and revision received Mar. 7, 2005.